



An experimental study and FEM simulation on machining characteristics in high speed milling of Ti-6Al-4V alloy

A. Sreenivasa Rao^{1*}, K.Venkata Rao²

1 Department of Mechanical Engineering, MLR Institute of Technology, Hyderabad-500 043, Telangana, India.*

2. Department of Mechanical Engineering, Vignan's Foundation for Science Technology and Research University, Guntur-552213, A.P, India.

Received 15 Oct 2017,
Revised 07 May 2018,
Accepted 10 May 2018

Keywords

- ✓ Titanium alloy;
- ✓ Milling;
- ✓ Multi response optimization ;
- ✓ Response Surface Methodology ;
- ✓ Finite Element Method

* A.Sreenivasa Rao
asrao2k14@gmail.com
+918465022671

Abstract

In this paper, the multi response optimization studies of titanium alloys have been analyzed by Response Surface Methodology (RSM) and Finite Element Methods (FEM). The cutting speed, feed and depth of cut are taken as input parameters and surface roughness, vibrational amplitude, elastic recovery, cutting forces and tool wear have been considered as machining characteristics/responses of the end milling of Ti-6Al-4V. The design of experiments follows the orthogonal array of L27 to perform experiments at three levels of cutting speed, feed and depth of cut. Two fluted tungsten carbide end mills are used in machining of titanium alloy. The process parameters are optimized for smaller values of surface roughness, amplitude of cutter vibration, cutting forces and tool wear and larger values of elastic recovery. In this work, numerical simulation is also carried out to study the machining characteristics for all the experiments. Interaction effect of the process parameters on the responses is also studied. These experimental and numerical values have been correlated. This analysis is used in online tool condition monitoring which improves productivity, machining time and tool life.

1. Introduction

Titanium alloys are widely used in aerospace applications that demand a good combination of high strength, good corrosion resistance and low stress. The mechanical properties lead to challenges in machining operations such as high process temperature as well as rapidly increasing tool wear. The surface roughness, vibrations, elastic recovery, cutting forces and tool wear have been experimentally investigated and put into relationship with the process parameters under dry machining condition. The correlation among tool wear propagation, surface roughness, vibrations and cutting forces have been analyzed and discussed. The vibration of mill cutter is a result of relative motion between work piece and tool, is required to measure vibration of cutter as close as to machining.

The vibration increases with increase of feed and the surface roughness has found to increase as speed was increased [1]. There is a strong correlation between vibrations and surface roughness in turning process and the vibrations are minimum to reduce surface roughness and tool wear [2]. The measurement of spindle and tool vibration is more important for tool condition monitoring in high speed milling process [3]. The LDV is used to measure vibration of rotating work piece in boring of steels on horizontal computer numerical control (CNC) lathe machine [4]. The LDV is used as the vibration measurement by Doppler's shift of the laser radiation [5]. The finite element model predicts the stress and temperature distribution for optimization of the process and residual stresses in the joint [6]. The algorithm based system to select optimum parameters for reduction in production time in both conventional and high speed milling operations while ensuring optimal finishing conditions like less production time and maximum profit in manufacturing [7]. The maximum profit through optimization of cutting parameters in conventional and high speed milling processes [8]. The genetic algorithms

to select optimum cutting parameters in order to reduce production cost by improving tool life and the Zirconia toughened alumina ceramic cutting tool has more life and it is able to machine at lower production cost [9]. The RSM model is used to optimize cutting parameters for minimum surface roughness and amplitude of cutter vibration in a turning process [10]. The effect of cutting speed, feed rate and depth of cut on turning of hard material with cubic boron nitride tool and used RSM to predict surface roughness and a good correlation is found between them [11]. The potential functions of the body can predict the bulk modulus of aluminum simulation data from the FEM code LAMMPS in agreement with the experimental data [12]. The accurate value of surface roughness in turning of AISI 1019 steel and found feed as the influence parameter [13]. The increased cutting speed and feed rate leads to wear in cutting edges of the tool material [14]. The cutting speed has significant effect on the cutter vibration [15]. There is 6%-40% of energy savings can be achieved in metal cutting with optimum cutting parameters [16]. The evaluation of the amount and direction of spring back states that the larger elastic recovery is required for better tool life [17]. The correlation of vibrations during machining and three dimensional finite element simulations in tool wear monitoring of a metal turning operation [18]. A new analytical method for the prediction of cutting tool temperature in end milling and claimed the dramatic tool temperature variation in end milling can cause excessive tool wear and shorten its tool life especially in machining of hard materials [19].

The main objective of this work is to experimentally investigate the input parameters on machining characteristics/responses during milling of Ti-6Al-4V with carbide end mills under dry machining condition. The experimental and simulated values have been analyzed and discussed.

2. Materials and Methods

The experiments have been carried out on Chandra BFW CNC milling machine as shown in the Figure 1. The following procedure was used to carry out the experiment under dry condition. Each trail was started with a new end mill with one new test condition (trail) and machining was stopped at the end of each pass. An LDV was placed in front of the machine and the LDV produces a laser beam to the rotating mill cutter to measure vibration signals and the setup of experiment is shown in the Figure 1.



Figure 1: Three axis CNC vertical milling machine with Laser Doppler Vibrometer (LDV)

After each pass, the work piece was removed and its surface roughness, amplitude of vibrations, elastic recovery, tool wear and cutting forces are measured. The above steps were repeated and remained the same in the experiment with a new end mill. The experimental and simulated data of 27 experiments have been tabulated in Table 1. The surface roughness of the work piece was measured by a diamond tipped stylus instrument. To measure surface roughness of the work piece, the cut off length was taken as 40mm and the sampling length as 100mm. The cutting forces are measured by dynamometer and tool wear and elastic recovery is measured by Scanning Electron Microscope. Samples of Ti-6Al-4V with dimensions of 100mm X 100mm X 10mm have been tested. Three levels of cutting speed (95, 110 and 126 m/min), three levels of feed rates (0.1, 0.2 and 0.3mm/rev) and three levels of depth of cut (0.3, 0.6 and 1mm) have been taken into account. The machined sample of work piece is shown in Figure 2.

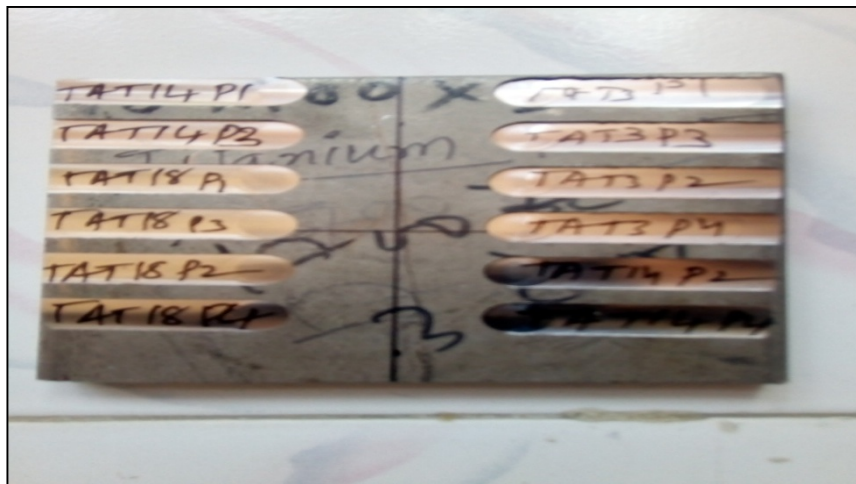


Figure 2: The machined titanium alloy work piece

3. Results and Discussion

The experimentation has been performed in random sequence, in order to reduce the effect of any possible error. The titanium sample is fixed in a vice and the Laser Doppler Vibrometer (LDV) is used to measure vibrations through data logger. As per Taguchi design of experiments (DOE), total 27 experiments have been performed on a machine with experimental and simulated results shown in the Table 1.

Table 1: The DOE with experimental and simulated values of responses of the material Ti-6Al-4V

Exp. No.	Design of experiments			Experimental Values of Responses						Simulated Values of Responses					
	C S (m/min)	FR (mm/rev)	DOC (mm)	Ra (μm)	V _x (μm)	V _y (μm)	S (μm)	V _B (μm)	F N	Ra (μm)	V _x (μm)	V _y (μm)	S (μm)	V _B (μm)	F N
1	95	0.1	1.0	1.2	7.22	5.7	0.15	0.17	748	1.16	7.08	5.77	0.153	0.167	739
2	95	0.2	1.0	0.98	7.22	5.6	0.14	0.17	582	0.99	7.11	5.68	0.15	0.177	572
3	95	0.3	1.0	1.08	7.23	5.47	0.153	0.17	688	1.1	7.12	5.53	0.158	0.177	675
4	95	0.1	0.6	0.66	6.73	5.59	0.132	0.204	581	0.69	7.06	5.43	0.137	0.207	592
5	95	0.2	0.6	1.35	6.7	5.45	0.133	0.188	812	1.37	6.7	5.72	0.13	0.193	798
6	95	0.3	0.6	1.73	7.13	5.76	0.177	0.179	907	1.74	7.46	5.77	0.182	0.187	893
7	95	0.1	0.3	0.59	6.92	5.47	0.14	0.275	546	0.61	6.59	5.7	0.138	0.287	529
8	95	0.2	0.3	1.16	6.03	5.69	0.157	0.235	1042	1.22	6.03	5.82	0.159	0.246	1059
9	95	0.3	0.3	1.33	6.29	5.73	0.167	0.183	513	1.27	6.37	5.77	0.174	0.187	500
10	110	0.1	1.0	1.18	7.19	5.77	0.147	0.17	896	1.16	6.85	5.85	0.152	0.173	880
11	110	0.2	1.0	1.13	7.22	5.63	0.143	0.183	913	1.18	6.89	5.68	0.147	0.183	902
12	110	0.3	1.0	1.82	7.15	5.24	0.141	0.17	680	1.89	7.2	5.27	0.145	0.167	672
13	110	0.1	0.6	0.99	6.52	5.53	0.135	0.275	569	1.02	6.55	5.71	0.141	0.283	559
14	110	0.2	0.6	0.98	6.67	5.27	0.142	0.21	733	1.00	6.38	5.33	0.142	0.21	720
15	110	0.3	0.6	1.74	6.75	5.42	0.16	0.18	915	1.81	6.88	5.62	0.162	0.183	900
16	110	0.1	0.3	0.57	6.06	5.48	0.13	0.279	519	0.6	6.09	5.54	0.136	0.287	508
17	110	0.2	0.3	0.87	5.96	5.21	0.15	0.27	1102	0.85	5.73	5.34	0.147	0.277	1109
18	110	0.3	0.3	1.24	6.29	5.45	0.17	0.24	467	1.25	6.12	5.51	0.175	0.25	456
19	126	0.1	1.0	1.55	6.54	5.64	0.14	0.194	1010	1.61	6.41	5.77	0.147	0.2	1007
20	126	0.2	1.0	1.46	6.76	5.73	0.14	0.187	944	1.41	6.8	5.75	0.136	0.187	934
21	126	0.3	1.0	1.51	6.99	5.55	0.13	0.173	950	1.48	7.15	5.63	0.126	0.173	937
22	126	0.1	0.6	1.38	6.43	5.49	0.13	0.278	442	1.35	6.39	5.71	0.127	0.277	431
23	126	0.2	0.6	1.05	6.74	5.57	0.134	0.267	845	1.02	7.08	5.7	0.137	0.27	836
24	126	0.3	0.6	1.56	6.67	5.34	0.14	0.207	920	1.57	6.68	5.42	0.134	0.217	910
25	126	0.1	0.3	1.00	6.47	5.74	0.145	0.27	520	0.96	6.79	5.92	0.152	0.263	511
26	126	0.2	0.3	0.83	6.43	4.79	0.138	0.28	471	0.84	6.17	4.71	0.144	0.28	462
27	126	0.3	0.3	1.71	6.67	5.06	0.16	0.246	498	1.67	6.55	5.25	0.164	0.243	487

In each experiment, surface roughness, cutter vibrations, elastic recovery, tool wear and cutting force on machined surface were measured. The analysis of responses is done by response surface methodology and finite element methods. In this work, LDV was used for online acquisition of cutter vibration data in the form of AOE signals as shown in the Figure 3.

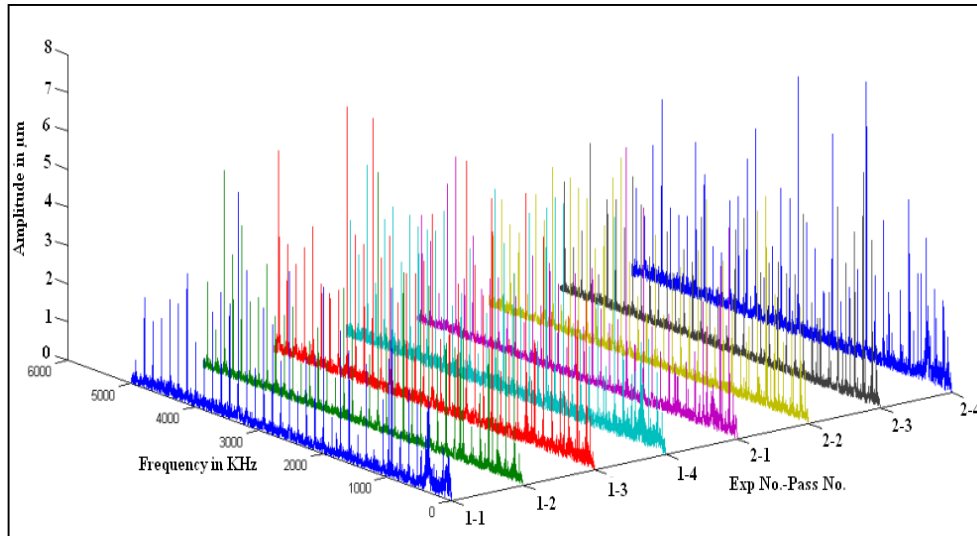


Figure 3: Frequency domains for the experiment 1 and 2

The optimum values of surface roughness and amplitude of cutter vibrations and elastic recovery are predicted by using response surface methodology and the tool wear and cutting force by Deform 3D. The elastic recovery of a work piece and tool wear of the end mill is measured by SEM is shown in the Figure 4.

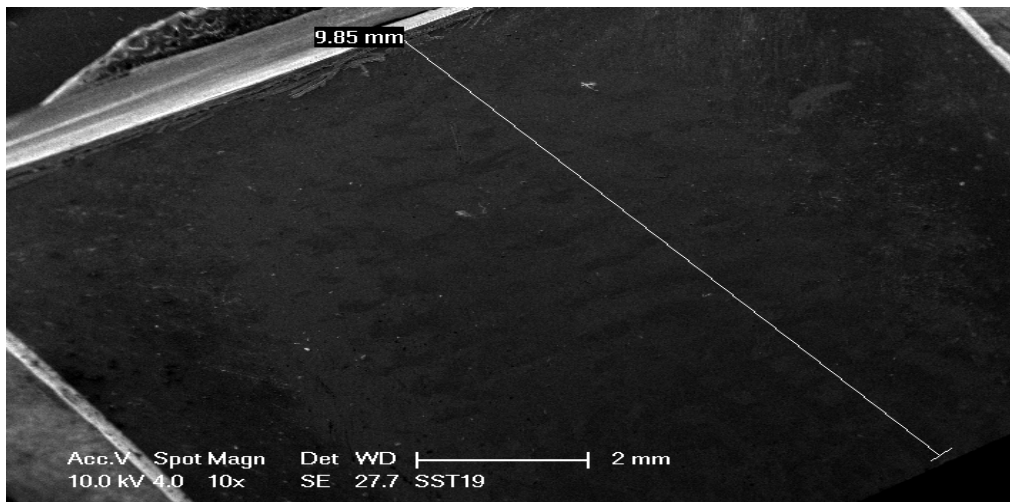


Figure 4: Measurement of elastic recovery of a titanium alloy sample using SEM

In this study, smaller the better function was used for surface roughness, amplitude of cutter vibrations, cutting forces and tool wear and larger the better function for elastic recovery because these responses should be optimum for any product to obtain good product quality and tool life.

3.1 Effect of Process parameters on R_a using Design Expert V 6.1

Interaction effect of cutting speed, feed rate and depth of cut on the amplitude of cutter vibration in feed direction is shown in the Figure 5. The Figure 5 (a) represents normal probability plot of the residuals for the surface roughness, most of the residuals are almost close to the straight line. That indicates that there is normal distribution of errors for the surface roughness.

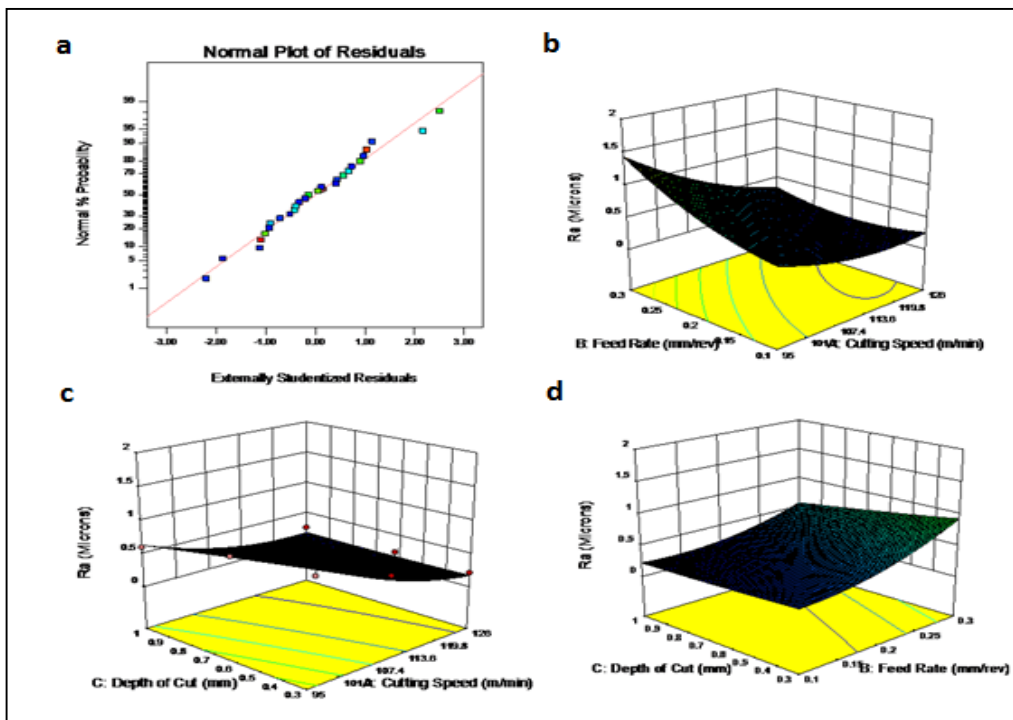


Figure 5: (a) Normal probabilities of residuals for R_a . (b) Effect of feed and cutting speed on R_a , (c) effect of depth of cut and cutting speed on R_a , and (d) effect of depth of cut and feed rate on R_a

As per the Figures 5 (b), the surface roughness is found to be lower at 113.6m/min of cutting speed and 0.25 mm/rev of feed rate. If feed rate increases, the surface roughness will also increase. If the cutting speed increases, the surface roughness will also increase. When the cutting speed is above 113.6m/min, the surface roughness will also increase. When the feed rate is above 0.25mm/rev the surface roughness will also increase. As per the Figure 5 (c and d), it is observed that when the feed rate is at 0.18mm/rev and depth of cut at 0.6 mm, the surface roughness is low. When the depth of cut is above 0.6 mm and feed rate is at 0.3mm/rev the surface roughness is high.

3.2 Effect of parameters on V_x

Interaction effect of cutting speed, feed rate and depth of cut on the amplitude of cutter vibration in feed direction is shown in the Figure 6. The Figure 6 (a) represents normal probability plot of the residuals for the amplitude in feed direction, most of the residuals are almost close to the straight line. That indicates that there is normal distribution of errors for the amplitude in feed direction. As per the Figures 6 (b), when the feed rate and cutting speed increases, the amplitude of cutter vibration will increase. It is also observed that at high feed rates and low cutting speeds, the amplitude of cutter vibration is very high. As per the Figure 6 (c and d), the amplitude is found to be higher at 1mm of depth of cut and cutting speed of 95 m/min. The amplitude of cutter vibration is getting lower when the depth of cut decreases. When the depth of cut 0.3 mm, cutting speed 95m/min and the feed rate 0.1mm/rev where the amplitude of cutter vibration is very low. When the depth of cut t 1mm, which gives higher amplitude of cutter vibration. The higher depth of cut is a significant parameter on cutter vibrations. There is no significance of cutting speed and feed rate on the amplitude of cutter vibration in feed direction. Among the cutting speed, feed rate and depth of cut, the feed rate has significant effect on the vibration.

3.3 Effect of Parameters on V_y

Interaction effect of cutting speed, feed rate and depth of cut on the amplitude of cutter vibration in depth of cut direction is shown in the Figure 7. The Figure 7 (a) represents normal probability plot of the residuals for the amplitude of cutter vibration in depth of cut direction, most of the residuals are almost close to the straight line. This indicates that there is normal distribution of errors for the amplitude of cutter vibration along y direction.

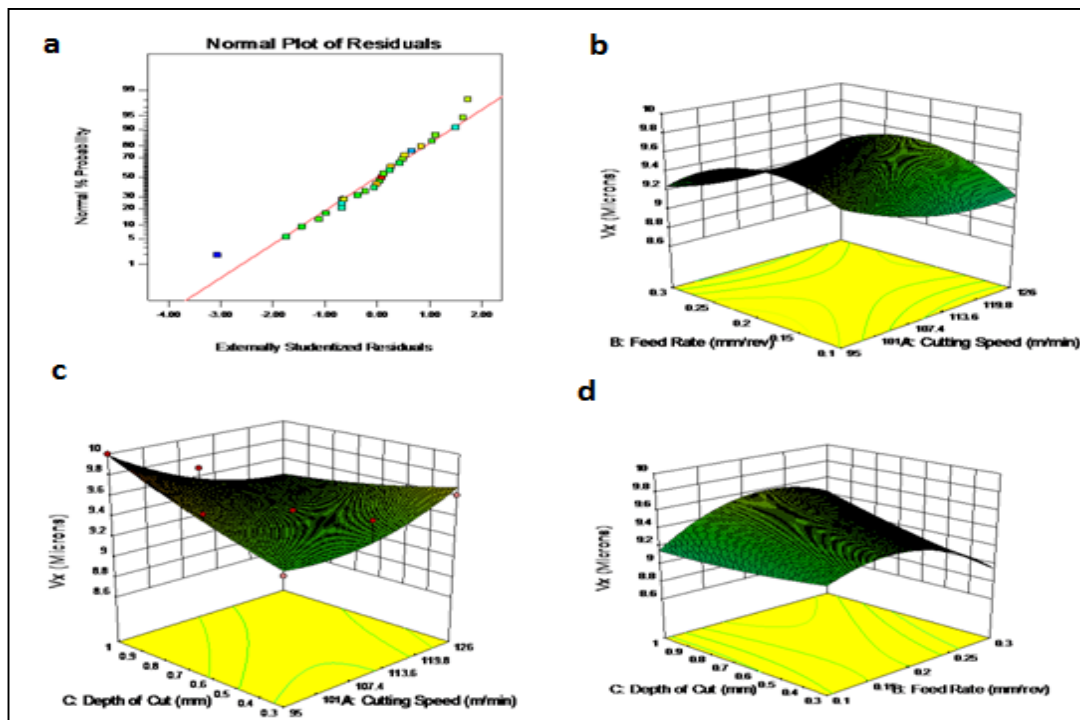


Figure 6: (a) Normal probabilities of residuals for V_x (b) Effect of feed and cutting speed on V_x , (c) Effect of depth of cut and cutting speed on V_x , and (d) Effect of depth of cut and feed rate on V_x .

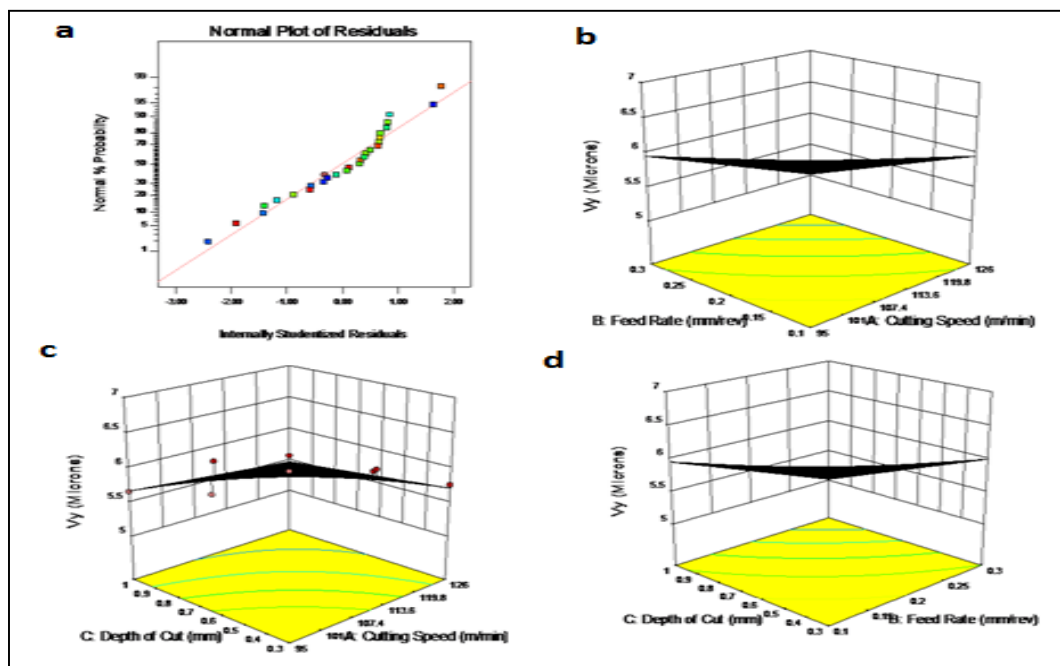


Figure 7: (a) Normal probabilities of residuals for V_y (b) Effect of feed and cutting speed on V_y , (c) Effect of depth of cut and cutting speed on V_y , and (d) Effect of depth of cut and feed rate on V_y .

As per the Figures 7 (b,c,d), When the feed rate 0.3mm/rev and cutting speed 95 m/min where the V_y is high. At same time it is observed that at feed rate 0.3mm/rev and cutting speed 95m/min, the V_y is low. At the depth of cut 1mm and cutting speed at 95m/min the V_y is high. The depth of cut 0.3mm and feed rate 0.3mm/rev, the V_y is high.

3.4 Effect of Parameters on ‘S’

Interaction effect of cutting speed, feed rate and depth of cut on the elastic recovery is shown in the Figure 8.

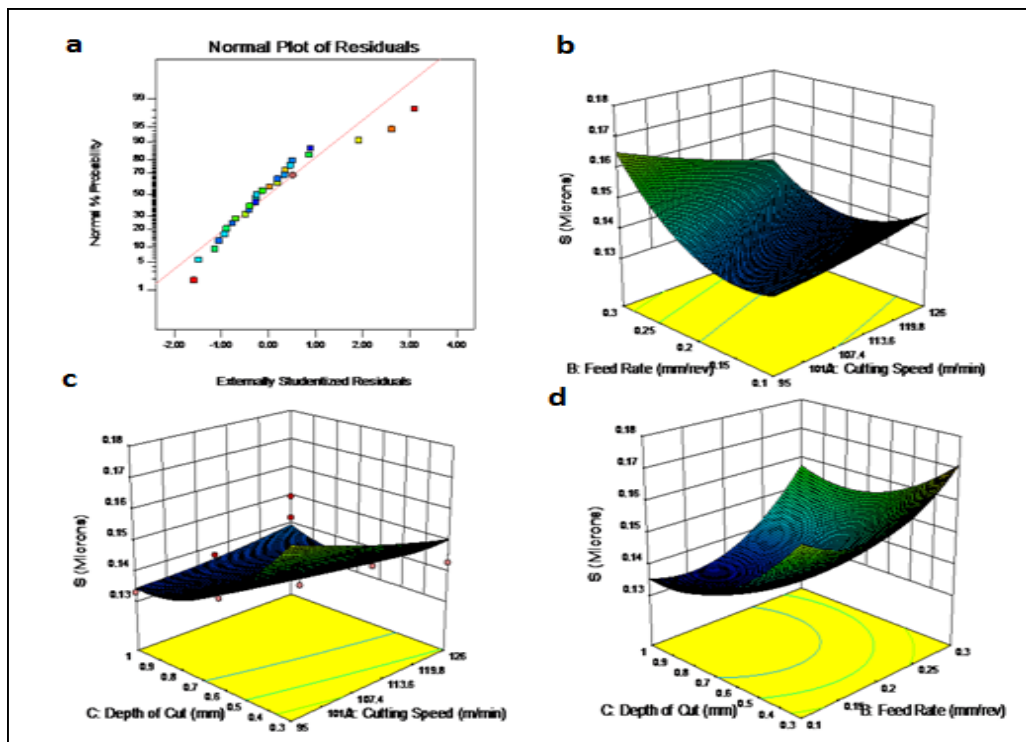


Figure 8: (a) Normal probabilities of residuals for ‘S’ (b) Effect of feed and cutting speed on ‘S’, (c) Effect of depth of cut and cutting speed on ‘S’, and (d) Effect of depth of cut and feed rate on ‘S’

The Figure 8 (a) represents normal probability plot of the residuals for the elastic recovery, most of the residuals are almost close to the straight line. That indicates that there is normal distribution of errors for the elastic recovery of the material. As per the Figure 8 (b), the feed rate 0.3 mm/rev and cutting speed 95m/min where the elastic recovery is high. At the feed rate 0.1mm/rev and cutting speed 95m/min where the elastic recovery is very low. As per the Figure 8 (c and d), the depth of cut 1mm and cutting speed 95m/min where the elastic recovery is lower. The feed rate 0.3mm/rev and depth of cut 0.3 mm where the elastic recovery is higher.

The cutting speed and depth of cut have a significant contribution in high elastic recovery of the materials. Based on the experimental results, four factor interaction response function for elastic recovery, surface roughness and vibrations along x and y can be expressed as function of process parameters. The quadratic model for the elastic recovery is given by the following equation (1):

$$S = 0.27847 - 9.20921E - 004v + 0.017955f - 0.24799d - 3.94475E - 003vf + 9.21643E - 004vd + 0.10360fd + 4.30108E - 006v^2 + 1.06111f^2 + 0.073280d^2 - (1)$$

3.5 Finite Element Analysis for Ti-6Al-4V by using DEFORM 3D

The 3D model in DEFORM 3D is reported in the Figure 9, where it is possible to see the cutting forces in Y direction. In the present work, the cutting tool assumed to be as rigid object meshed with more than 50000 elements is as per the cutting angles set in experiment and it moves in a linear direction.

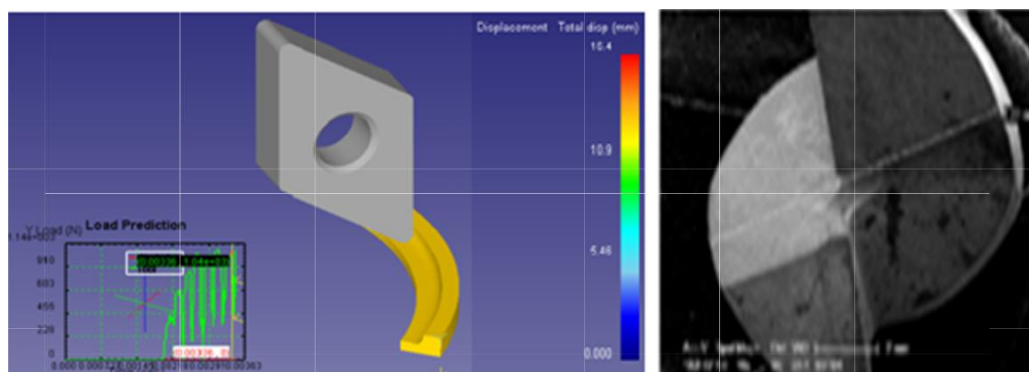


Figure 9: Cutting force and tool wear simulation at V=126m/min, f=0.3mm/rev and d=1mm and corresponding tool wear

The work piece is considered as a rigid elastic plastic object meshed with more than 25000 elements and it cannot move. The friction is modeled as a shear factor of 0.6. The base of the work piece is constrained in all directions. The tool is subjected to move in Y direction at three different constant speeds and constrained against movements in X and Z directions. The DEFORM 3D is used to conduct the FEM simulation for machining by considering two flute tungsten carbide end mill geometry is implemented in the model. In this work, FEM has been carried out for 27 cases of experiments consisting of three different feed rates, cutting speeds and depth of cuts. The experimental and numerical values at different test cutting conditions have been tabulated in Table 1. Based on the simulation, the cutting speed plays a major role in increment of cutting forces. The cutting force 'F' has a higher value at cutting speed 110 /min, feed rate 0.2 mm/rev and 0.3 mm depth of cut. The cutting force 'F' has a lower value at cutting speed 126 m/min, feed rate 0.1 m/rev and 0.6 mm depth of cut. The tool wear is higher at cutting speed 126m/min, feed rate 0.1 mm/rev and 0.3 mm depth of cut. The tool wear is lower at cutting speed 95m/min, feed rates at 0.1 mm/rev, 0.2 mm/rev and 0.3 mm/rev and at depth of cut 1mm. Based on the simulation and experimentation, the feed rates have no significant effect on tool wear.

Conclusions

The optimization of cutting parameters is to improve surface quality and tool life is found by using multi response optimization technique. RSM and FEM simulations are used to study and identify the cutting parameters which affect the surface roughness, vibrations, tool wear, elastic recovery and cutting forces in machining.

The cutting speed, feed rate and depth of cut are found to be significant cutting parameters on output responses have been proved. The multi response optimization technique shows at a particular cutting speed, feed rate and depth of cut are the optimal combination of milling parameters for lower values of surface roughness, tool wear, vibrations and cutting forces with higher values of elastic recovery has been proved in our study. The numerical simulation gives good results and minimizes the cost of experimentation on machining of titanium alloys in high speed milling process. The error between the numerical and experimental values for all responses is within the prescribed limit.

Acknowledgement-This work is funded by Science and Engineering Research Board, Department of Science and Technology, Government of India. Grant No.: SERB/F/1761/2015-16. Dr. K Venkata Rao is Principal Investigator of the Project and co author of the manuscript.

References

1. G.H.V. Prasadbabu, B.S.N. Murthy, K. Venkatarao, C. Ratnam, *Proc I Mech E Part B: J Engineering Manufacture* 1 (2016) 1–10
2. E.D. Kirby, J.C. Chen, J.Z. Zhang, *Expert. Syst. Appl.* 30 (2006) 592–604.
3. K. Tatar, P. Gren, *Int. J. Mach. Tool. Manu* 48 (2014) 380–387.
4. K. Venkatarao, B.S. Murthy, N. Mohanrao, *Measurement* 46 (2013) 4075–4084.
5. D. Bartout, N. Suleymanon, *J. Mater. Environ. Sci* 8 (2017) 4426-4433
6. M. Alberti, J. Ciurana, M. Casadesu's, *J. Mater. Process. Tech* 168 (2005) 25–35.
7. N. Baskar, P. Asokan, R. Saravanan, *J Mater. Process. Tech.* 174 (2006) 239–249.
8. A. Senthil Kumar, M. Adam Khan, R. Thiraviam, *Mach. Sci. Technol.* 10 (2006) 471–489.
9. Y. Sahin, *J. Mater. Process. Tech* 209 (2009) 3478–3489.
10. G. Amit Kumar, *Int. J. Prod. Res.* 48 (2010)763–778.
11. Y. Sahin, A. R. Motorcu, *Int. J. Refract. Met. H.* 26 (2008)284–290.
12. H. Chabba, M. Lemmalem, A. Derouiche, D. Dafir, *J. Mater. Environ. Sci* 9 (2018) 93-99
13. B. Bhardwaj, R. Kumar, P.K. Singh, *Proc I Mech E, Part B: J Engineering Manufacture* 228 (2014)223-232
14. L. M. Maiyar, R. Ramanujam, K. Venkatesan, *Proc. Eng;* 64 (2013)1276–1282.
15. N. Muthukrishnan, J.P. Davim, *J. Mater. Process. Tech* 209 (2009) 225–232.
16. H. S. Sodhi, D.P. Dhiman, R.K. Gupta, *Int J. Appl. Eng. Res* 7 (2012) 44–54.
17. S. T. Newman, A. Nassehi, R. Imani Asrai, *CIRP J. Manuf. Sci. Techn* 5 (2012) 127–136.
18. D. B. Zhu, L. Ma, D.C. Li, B.H. Lu, *Mech. Sci. Technol.*,19 (2000) 953-955
19. B. S. Prasad, M. Prakash Babu, Y. Rama Mohana Reddy, *Proc I Mech E Part B: J. Engineering manufacture* 230 (2016)203-214

(2018) ; <http://www.jmaterenvironsci.com>